Biogeosciences Discuss., 12, 4907–4945, 2015
www.biogeosciences-discuss.net/12/4907/2015/
doi:10.5194/bgd-12-4907-2015

Biogeosciences
Discussions
Open Access

Macroalgae contribute to nested mosaics of pH variability in a sub-Arctic fjord

D. Krause-Jensen[1,2], C. M. Duarte[3,4], I. E. Hendriks[5], L. Meire[6,7], M. E. Blicher[6], N. Marbà[5], and M. K. Sejr[1,2]

[1]Arctic Research Centre, Bioscience, Arhus University, C. F. Møllers Allé 8, 8000 Århus C, Denmark
[2]Department of Bioscience, Arhus University, Vejlsøvej 25, 8600 Silkeborg, Denmark
[3]Red Sea Research Center, King Abdullah University of Science and Technology, Thuwal 23955-6900, Kingdom of Saudi Arabia
[4]Faculty of Biosciences, Fisheries and Economics, University of Tromsø, Tromsø, Norway
[5]Department of Global Change Research, IMEDEA (CSIC-UIB) Instituto Mediterráneo de Estudios Avanzados, Miquel Marqués 21, 07190 Esporles, Spain
[6]Greenland Climate Research Centre, Greenland Institute of Natural Resources, Kivioq 2, Box 570, 3900 Nuuk, Greenland
[7]Marine Biology Laboratory, University of Ghent (UGent), Krijgslaan 281 (S8), 9000 Gent, Belgium

Received: 10 February 2015 – Accepted: 3 March 2015 – Published: 27 March 2015

Correspondence to: D. Krause-Jensen (dkj@bios.au.dk)

Published by Copernicus Publications on behalf of the European Geosciences Union.

Abstract

The Arctic Ocean is considered the most vulnerable ecosystem to ocean acidification (OA) and large-scale assessments of pH and the saturation state for aragonite (Ω_{arag}) indicate that it is already close to corrosive states ($\Omega_{arag} < 1$). In high-latitude coastal waters the regulation of pH and Ω_{arag} is far more complex than offshore because increased biological activity and input of glacial meltwater affect pH. As most calcifiers occupy coastal habitats, the assessment of risks from OA to these vulnerable organisms cannot be derived from extrapolation of current and forecasted offshore conditions, but requires an understanding of the regimes of pH and Ω_{arag} in their coastal habitats. To increase knowledge of the natural variability of pH in the Arctic coastal zone and specifically to test the influence of benthic vegetated habitats, we quantified pH-variability in a Greenland fjord in a nested scale approach. A sensor array logging pH, O_2, PAR, temperature and salinity was applied on spatial scales ranging from km-scale across the horizontal extension of the fjord, over 100 m scale vertically in the fjord, 10–100 m scale between subtidal habitats with and without kelp forests and between vegetated tidal pools and adjacent vegetated shores, to cm-m scale within kelp forests and mm-scale across boundary layers of macrophyte tissue. In addition, we assessed the temporal variability in pH on diurnal and seasonal scales. Based on pH-measurements combined with relationships between salinity, total alkalinity and dissolved inorganic carbon we also estimated variability of Ω_{arag}. Results show variability in pH and Ω_{arag} of up to 0.2–0.3 units at several scales, i.e. along the horizontal and vertical extension of the fjord, between seasons and on a diel basis in benthic habitats and within 1 m^3 of kelp forest. Vegetated intertidal pools exhibited extreme diel pH variability of > 1.5 units and macrophyte boundary layers a pH-range of up to 0.8 units. Overall, Ω_{arag} was favorable to calcification, and pelagic and benthic metabolism was an important driver of pH and Ω_{arag} producing mosaics of variability from low levels in the dark to peak levels at high irradiance. We suggest that productive coastal environments may form niches of high pH in a future acidified Arctic Ocean.

1 Introduction

The Arctic Ocean is considered to be the most vulnerable ecosystem to ocean acidification due to the combined effects of low temperature, which increases the solubility of CO_2 and, at places, dilution of the buffering capacity of seawater by freshwater inputs (Fabry et al., 2009; AMAP, 2013). Indeed, large-scale assessments of pH and the saturation state for aragonite (Ω_{arag}) indicate that Arctic Ocean seawaters are already in close proximity to corrosive states ($\Omega_{arag} < 1$, Fabry et al., 2009). However, whereas this has been documented for offshore waters, the Arctic contains a massive coastline, comprising about 35 % of the world's coastline (Krause-Jensen and Duarte, 2014) where the regulation of pH and Ω_{arag} is far more complex than that offshore (Hofmann et al., 2011; Duarte et al., 2013). In coastal waters, the role of air–sea CO_2 exchange in regulating pH operates along with watershed effects driven by the discharge of freshwater and the effects of metabolically intense communities on pH (Duarte et al., 2013). The Greenland Ice Sheet is melting at a rate that has more than doubled in the recent decade (Helm et al., 2014) and Greenland fjords are, hence, potentially among the most susceptible to the effects of freshening and acidification.

As most calcifiers occupy coastal habitats, the assessment of risks of Arctic acidification to these vulnerable species cannot be derived from extrapolation of the current and forecasted offshore conditions alone, but requires an understanding of the regimes of pH and Ω_{arag} in the coastal habitats they occupy. Such information is currently largely lacking for the Arctic in general and for Greenland in particular, which calls for efforts to understand variability of pH in the coastal zone informing on the factors controlling pH and ultimately determining the vulnerability of the coastal Arctic Ocean ecosystem to ocean acidification.

Greenland has a vast and highly indented coastline, extending along about 44 000 km and representing ca. 12 % of the world's coastline (Krause-Jensen and Duarte, 2014). This coastline forms a complex network of fjords and open coasts that contains multiple features contributing to heterogeneity, such as continental ice and freshwater discharge at the headwaters, variable slopes and substrates, differential water residence time conducive to widely distinct temperature regimes within neighboring areas (Olesen et al., 2015), and tides that generate intertidal habitats and force flow patterns. In addition, Greenland fjords often support highly productive kelp forests (Krause-Jensen et al., 2012) and intertidal seaweed communities (Høgslund et al., 2014), which have been suggested to have the capacity to affect pH and Ω_{arag} locally (Krause-Jensen and Duarte, 2014) as demonstrated for subtropical and tropical vegetated habitats (e.g. Hofmann et al., 2011; Hendriks et al., 2014). Calcifiers such as bivalves, brittle stars and sea urchins are ecologically important as they contribute significantly to carbon cycling in both sub-Arctic and high-Arctic areas of Greenland where their distribution range from the intertidal zone to > 300 m depth (Sejr et al., 2002; Blicher et al., 2007, 2009, 2013; Blicher and Sejr, 2011). Calcifiers, especially bivalves are also important prey items for marine mammals (Born et al., 2003) and sea birds (Blicher et al., 2011).

Although the variability in pH and Ω_{arag} in Greenland fjords has not been reported, available oceanography and environmental surveys suggest that this may be substantial. For instance, in Young Sound, Sejr et al. (2011) found that the extent of sea-ice cover and inputs of glacial melt water affect seawater $p\text{CO}_2$ levels and sea–air exchange at spatial, seasonal and inter-annual scales. Seasonal dynamics of autotrophic and heterotrophic plankton metabolism have also been found to markedly affect $p\text{CO}_2$ levels in Kobbefjord, a sub-Arctic fjord in SW Greenland (Sejr et al., 2014). However, information on scales of variability in pH and Ω_{arag} in Greenland fjords is still lacking, precluding the assessment of their current and future vulnerability to ocean acidification.

Here we quantify pH variability in Kobbefjord, SW Greenland. This sub-Arctic fjord supports dense and productive subtidal kelp forests, intertidal macroalgal habitats and high abundance of bivalves and sea urchins with important roles in the ecosystem (Blicher et al., 2009; Krause-Jensen et al., 2012). We hypothesize that Kobbefjord contains a mosaic of pH environments nested across a range of scales of variability and that primary production in general, and by macroalgae in particular, may be an important driver of pH variability relevant for benthic calcifiers. We first assess seasonal and spatial variability in the pelagic pH at km scale along the horizontal extension and at 100 m scale vertically in the fjord. We then examine diel variability in pH within subtidal benthic habitats colonized by kelp forest or microalgae/scattered filamentous algae as well as in vegetated tidal pools and adjacent vegetated intertidal shores, with the distance between parallel deployments at the 10–100 m scale. We further explore the pH variability 3-dimensionally at cm- to m-scale within the kelp forest ecosystem and at mm-scale across the thallus boundary layer of key macrophyte species. Whereas our assessment focuses on pH, we also discuss the associated variability of Ω_{arag}.

2 Methods

2.1 Study area

Kobbefjord is located in the extensive Godthåbsfjord system in south west Greenland (Fig. 1a). The fjord is 17 km long and 0.8–2 km wide and has a maximum depth of 150 m. It is subjected to marked exchange of coastal water driven by a tidal range of 1–4.5 m (Richter et al., 2011) and receives freshwater mainly from a river in the innermost part of the fjord, leading to a salinity gradient in the surface water. Sea-ice usually covers the inner part of the fjord from December to early May, but the outer part of the fjord is permanently ice free. Whereas the phytoplankton community is the main primary producer in the central parts of the fjord (Sejr et al., 2014), subtidal macroalgae form productive benthic habitats along the shores to water depths of ca. 40 m (Krause-Jensen et al., 2012) interspaced with communities of benthic microalgae (Glud et al., 2010; Attard et al., 2014) as well as with scattered eelgrass meadows at 1–3 m depth (Olesen et al., 2015). Communities of intertidal macroalgae are prominent in the intertidal zone where they form an important habitat for e.g. blue mussel (Blicher et al., 2013).

Three field campaigns targeting seasonal- and fjord-scale variability in pH in the pelagic zone were conducted in the spring (19 April), mid-summer (18 July) and late summer (3 September) of 2013 (Fig. 1b). The late summer survey was associated with an intensive campaign (27 August–6 September 2013) exploring pH variability in shallow subtidal kelp habitats and neighboring habitats colonized by benthic microalgae and scattered filamentous algae (Fig. 1c). A final late summer campaign (22–30 August 2014) addressed pH variability in vegetated tidal pools and surface waters of adjacent vegetated shores (Fig. 1c). All pH data from fjord-scale to micro-scale are reported on the total pH scale.

2.2 Fjord and seasonal scale pH variation

To determine the large-scale spatial and seasonal variation in physical and chemical parameters in the water column of Kobbefjord, vertical profiles were measured at 11 stations located along a longitudinal gradient following the main central axis of the fjord on 19 April, 18 July, and 3 September 2013 (Fig. 1b). We used a Seabird CTD (SBE19plus) equipped with sensors for temperature, conductivity, fluorescence (Seapoint Chlorophyll Fluorometer), oxygen (SBE 43, Seabird) and pH (SBE18, Seabird). Alongside CTD profiles, water samples were collected using a 5 L Niskin bottle at 1, 5, 10, 20, 30, and 40 m depth. Water was collected for dissolved oxygen measurement using Winkler titration (Parsons et al., 1984) which was used to calibrate the CTD oxygen optode. The pH sensor was calibrated using NBS buffers and a seawater TRIS buffer prepared according to Dickson (2007). Unfiltered water was transferred to 150 mL borosilicate glass bottles for pH analysis. The samples were poisoned with a saturated mercuric chloride solution, cooled and stored in darkness until arrival. Back in the lab, pH was measured potentiometrically using a glass reference electrode (Orion, Ross Ultra pH/ATC Triode) calibrated with NBS buffers and a seawater TRIS buffer prepared according to Dickson (2007). The measurements were used to correct the offset of the SBE 18 pH measurements.

For estimation of the saturation state of aragonite (Ω_{arag}), samples for analyses of dissolved inorganic carbon (C_T) and total alkalinity (A_T) were collected at 5 stations on one occasion (3 September 2013). Triplicate 12 mL samples were collected at 5, 10, 20, 30, 40 m depth and near the bottom. Samples were carefully siphoned through tygon tubing from Niskin bottles to 12 mL septum-capped glass vial (exetainers) allowing the water to overflow for two volume changes. The samples were poisoned with 100 µL 5 % $HgCl_2$ to avoid biological alteration. C_T was analyzed with a C_T analyzer (AS-C3, Apollo Scitech Inc). The accuracy of the analysis was 2.4 $\mu mol\,kg^{-1}$ (average numerical deviation from the reference material value) and the precision was 1.4 $\mu mol\,kg^{-1}$ (average SD of triplicate samples). A_T was analysed on an alkalinity titrator, AS-ALK2 from Apollo Scitech with verification against the same certified reference material used for pH measurements or a Metrohm Titrando 808 by open cell titration (Dickson et al., 2007) using Batch 136 supplied by the Andrew Dickson lab at UC San Diego for verification. Average analysis accuracy was 2.9 $\mu mol\,kg^{-1}$ (average numerical deviation from the reference material value). Relationships between A_T and salinity (S) were used to verify the published relationship for the Godthåbsfjord system ($TA = 159 + 63S$, Meire et al., 2014) which was subsequently applied for calculation of A_T based on salinity data collected in April, July and September. Ω_{arag} was calculated from A_T and pH using the CO_2SYS excel programme version 2.1 (Pierrot et al., 2006) with the K1 and K2 constants from Mehrbach et al. (1973), as modified by Dickson and Millero (1987).

2.3 Small-scale and diurnal-scale pH variation

To measure small-scale and diurnal-scale variation in pH and physico-chemical variables in kelp forests and adjacent sub-tidal habitats colonized by microalgae and scattered filamentous algae we constructed four metal frames each measuring approximately 0.90 m × 0.90 m × 1.10 m. Each frame was equipped with instruments that allowed continuous measurements of temperature, salinity, water level, oxygen concentration, photosynthetically active radiation (PAR) and pH at ca 50 cm above the seafloor

Title Page
Abstract | Introduction
Conclusions | References
Tables | Figures
◀| |▶
◀ ▶
Back | Close
Full Screen / Esc
Printer-friendly Version
Interactive Discussion

(Fig. 1s). Measurements were made every 10 min or less. We conducted 3 parallel deployments of two frames in kelp habitats and two frames in habitats colonized by microalgae and scattered filamentous algae, with each deployment lasting about 48 h. The typical distance between the frames in each habitat was 10–20 m and between kelp forests and habitats colonized by microalgae and scattered filamentous algae approximately 100 m. Conductivity, temperature and water level were measured using two Hydrolab DS5X and MicroCats (SBE37 Seabird). Oxygen concentration was measured using MiniDot oxygen loggers, Precision Measurement Engineering, and Hydrolab DS5X. PAR was measured using Odyssey PAR loggers from Dataflow Systems Pty Limited. pH was measured using Hydrolab DS5X and SeaFet pH loggers from Satlantic. Hydrolab DS5X pH sensors were calibrated with a routine two-point calibration using NIST buffers of pH_{NBS} 7.0 and 10.0. Before and after each deployment all instruments were placed in a 50 L tank with sea water to intercalibrate sensors. All pH loggers were offset to the same newly calibrated high-precision seafet pH sensor, calibrated at the Satlantic facility (www.satlantic.com) on the total scale using single-point calibration. Oxygen sensors were calibrated to O_2 concentrations of the tank as determined from Winkler titrations.

To monitor three-dimensional pH variations on a m-scale within the kelp canopy, we deployed a custom built multi-sensor array, consisting of an autonomous data logger (Datataker DT85, serial number 096 831) in a water-tight housing (custom built by Albatros Marine Technologies S.I.) with 16 pre-amplified pH electrodes (Omega, PHE-1304-NB). The pH sensors were attached to the submersible logger by 5 m long cables to allow for adjusting their position as needed (Fig. A1). The sensors were configured in-situ in a three dimensional array on the metal frame occupying a volume of approximately 1 m^3, with 4 sensors at 0.1 m from the bottom, 4 sensors at 0.2 m, 4 sensors just underneath the canopy and 4 above the canopy, which typically extended about 0.75 m above the seafloor. All pH sensors were calibrated with a three point calibration using NIST buffers of pH_{NBS} 4.0, 7.0 and 10.0 allowing at least 5 min between every reading for the sensors to stabilize. All pH loggers were offset to the same newly calibrated high-precision seafet pH sensor as mentioned above. On several occasions triplicate samples for determination of C_T and A_T were collected and analyzed as described above to allow calculation of carbonate chemistry and Ω_{arag}.

pH-variation in vegetated tidal pools and adjacent intertidal habitats on the shore were quantified over a diurnal cycle through sampling at low tide just after pool formation and prior to pool inundation during day and night. pH and Ω_{arag} were calculated from C_T and A_T samples collected and analyzed as described above and computed using the CO2SYS program (Pierrot et al., 2006) with in situ information on temperature and salinity. Salinity was analysed from water samples based on measurements of conductivity (Orion 3 STAR Conductivity benchtop) while oxygen concentration and water temperature were determined using a portable meter (Hack, HQ40d).

2.4 Micro-scale pH variation

pH-variations at a millimeter scale were measured in the laboratory on 6 different species of macrophytes (*Ascophyllum nodosum, Fucus vesiculosus, Saccharina longicruris, Agarum clathratum*, *Ulva lactuca*, *Zostera marina*) occurring in Kobbefjord and collected either there or, for logistic reasons, in another branch of the Godthåbsfjord system. From each species, a piece of approximately 5 cm × 2 cm was cut and mounted on a microscope slide in an aquarium with seawater before measurements. The set-up was mounted in a room with climate control and temperature was kept at 2–3 °C. We measured pH from a point close to the leaf surface up until out of the diffusive boundary layer (DBL) where the pH was stable. We used UNISENSE micro-pH sensors with 25 or 50 µm tips, connected to a Volt meter with 1 decimal precision for mV measurements (Consort, R362). pH sensors were calibrated with a three point calibration using NIST buffers of pH_{NBS} 4,0; 7,0 and 10,0 allowing at least 5 min between every reading for the sensor to stabilize. A USB microscope (Dinocapture) connected to a PC with on-screen visualization software aided in visually establishing the lowest point of the measurements, as close to the macrophyte surface as possible without breaking the tip of the electrode. A scaled picture from this lowest point allowed for back calculating the actual distance to the leaf surface afterwards. We allowed readings at this lowest point to stabilize for > 5 min after which the mV value was written down manually. The microsensor was then raised 20 µm with a precise 1-D micromanipulator, afterwards 30 µm, after which we continued with 50 µm increments and then 100 and 500 µm increments until a stable pH was obtained for 3 measurements or more and we considered we were outside the DBL. We evaluated 3 replicas of each species at a light intensity of 200 µmol photons $m^{-2}\,s^{-1}$, and calculated the ΔpH across the boundary layer (defined from the tissue surface to where pH was at 0.99 × water-column pH).

3 Results

3.1 Fjord-scale and seasonal pH variability

Large seasonal and spatial variability was observed in pH-values along the longitudinal gradient centrally in the fjord (Fig. 2a). pH_T in surface water increased in April due to CO_2 consumption by the spring bloom as evidenced by a very high fluorescence (Fig. A2), to a maximum value of almost 8.50, most pronounced in the mouth of the fjord with values of around 8.25 in the inner part (Fig. 2). Accordingly, a horizontal gradient of around 0.25 pH units was observed along the main axis of the fjord. pH_T values in upper layers decreased during the summer to around 8.35 in July and with the maximum observed towards the inner part of the fjord. A further decrease in pH was observed in September, with more homogenous values in surface waters along the fjord gradient resulting in a horizontal range of only 0.05 pH units. Vertical gradients in pH from the surface to the deeper waters of the fjord ranged from only 0.1 units in April, when the fjord was vertically mixed, over 0.15 units in September to 0.25 pH units in July when maximum pH_T values of 8.35 occurred in a subsurface algal bloom in the inner parts of the fjord with waters supersaturated in oxygen (up to 120 % saturation, Figs. A2 and A3) and minimum values of pH_T 8.1 were measured in the deeper sectors (Fig. 2a). Seasonally pH varied between 0.2 and 0.3 units in both surface and deep waters over the 5 months. Corresponding Ω_{arag} values ranged from minimum values of 1.5, observed in the bottom waters of the inner part of the fjord in July and September, to maximum values of 3, observed in the surface and subsurface waters in April and July (Fig. A4).

Oxygen saturation at the fjord-scale ranged greatly from 85 to 127 % and was strongly related to pH for each of the three periods (Fig. 3a), pointing at strong biological control of pH variability within the fjord. The slope of the pH vs. O_2 relationship was steepest for the April survey when the highest pH levels were observed. Examination of pH values in relation to fluorescence and temperature also showed that the warmest waters, of up to 10 °C, observed in July, supported intermediate pH, while the highest pH was observed in the coldest waters, corresponding to the April survey when temperatures were uniformly low across the fjord (Fig. 3b). On a vertical scale, the cold bottom waters with low fluorescence generally supported the lowest pH values across seasons. Hence, overall, pH showed much tighter correlation with O_2 levels than with water temperature, and the correlation between pH and O_2 was matched by a close correlation between Ω_{arag} and O_2-levels (Fig. 3c).

3.2 Small-scale and diurnal pH- variability in kelp forests and benthic habitats colonized by microalgae/scattered filamentous algae

The 3 parallel deployments in kelp forest and habitats colonized by microalgae and scattered filamentous algae encompassed 6 complete diurnal cycles which exhibited peak pH_T-levels during the day of 8.11 (8.04–8.19) (avg.(SD)) and of 8.08 (8.02–8.16), respectively, as opposed to minimum pH_T-levels during night of 8.02 (7.97–8.06) and 8.01 (7.94–8.09), respectively, with no significant difference between habitats (t test, $p > 0.05$). The diurnal range of minimum night pH to maximum day pH was slightly higher in the kelp forest (avg. ± SD = 0.098 ± 0.061) than above the microalgae/filamentous algae (0.073 ± 0.052) (paired, one-tailed t test, $p = 0.041$).

There were large differences in the extent of diel fluctuations in pH among deployments dependent on incident irradiance and the shifting phase of tidal state and the solar cycle (Fig. 4). Diel pH fluctuations were small during dark, cloudy days and when high tide coincided with peak solar radiation, thereby reducing incident irradiance on the benthic habitat. In contrast, diel pH fluctuations were amplified in deployments during sunny days when low tide coincided with peak solar radiation (Fig. 4). Hence, the interaction between tide and the solar cycle controlled incident radiation and thereby induced fluctuations in photosynthetic activity and pH. This was particularly apparent in kelp forests where peak daily pH increased as a function of maximum daily photosynthetic solar radiation reaching the habitat during the day whereas this relationship was not significant in the water column above the microalgae/filamentous algae (Fig. 5). Indeed, biologic control of pH was also reflected in strong relationships between pH and O_2 concentration within each deployment in the kelp forests ($R^2 = 0.64$–0.76) particularly during high irradiance, as opposed to weaker pH vs. O_2 relationships for the microalgae/filamentous algae sites ($R^2 = 0.05$–0.15) which also showed much smaller variability in O_2 levels (98–114 % saturation) than did the kelp forest (92–128 % saturation) (Fig. 6). The diurnal range of O_2 concentrations in the kelp forest matched the range recorded at pelagic fjord-scale on a seasonal basis (85–127 %, Fig. 3).

Changes in water masses by the tide, reflected by changes in salinity and temperature, also contributed to variations in pH and O_2 levels. This was visible as incidences of sudden changes in pH paralleling fluctuations in salinity and also as differences in pH levels between deployments in water masses of different salinity (Fig. 4). However, salinity explained much less of the variation in pH than did O_2, except in one deployment in the microalgae/filamentous algae habitat when salinity explained 51 % of the variation in pH as opposed to 15 % explained by O_2 ($R^2 = 0.04$–0.33 in kelp forest; $R^2 = 0.04$–0.51 in microalgae/filamentous algae, data not shown). So, overall biological activity had a much stronger influence on pH than had exchange of water masses.

The observed diurnal pH variability also translated into important fluctuations in Ω_{arag}, involving 0.18 ± 0.06 units (from max night levels of 1.77 ± 0.21 to min day levels of 1.60 ± 0.17) in the kelp forest and $0.14 \pm 0.07 \Omega_{arag}$ units (from max night levels of 1.72 ± 0.30 to min day levels of 1.58 ± 0.26) at the microalgae/filamentous algae sites.

3.3 Meter to millimeter-scale pH variability in kelp forests

Examination of the variability in pH within 1 m^3 kelp forest, sampled from the bottom of the canopy to the overlying water column, using the multi-electrode array, showed very large concurrent pH variability involving about 0.2 to 0.3 pH unit differences at any given time and with a total pH_T range of 7.76–8.36 across deployments (Fig. 7). In general, pH tended to be highest at the top of the canopy and in the water just above the canopy, reflecting that the canopy top is the most photosynthetically active layer, while pH was generally lower in the shaded bottom part of the canopy (Fig. 7) where photosynthetic biomass and incident light are lower and respiration rates higher. The range of pH within 1 m^3 of kelp forest at any one point in time was comparable among deployments, despite the different light conditions, although the absolute values of pH differed among deployments with highest levels observed at peak incident light (Fig. 7). This small-scale variability in pH also translated into a variability in Ω_{arag} of about 0.20 units in 1 m^3 of habitat at any time.

pH also varied significantly within the boundary layer of the six macrophyte species examined in the light (Fig. 8a), with pH increasing by 0.07–0.85 units, depending on species, from the top of the 0.3–2.2 mm thick boundary layer to the surface of the plants (Fig. 8b). There were important differences among species, which likely related to their photosynthetic rates and variations in the thickness of their boundary layer.

3.4 pH variability in intertidal pools

pH and oxygen concentration showed important diel variability in vegetated intertidal pools, with oxygen super-saturation (up to 176 %) during the day and under-saturation (down to 11 %) at night, compared to far more uniform concentrations in the surface waters on the adjacent vegetated shore (89–111 % saturation, Fig. 9). Accordingly, pH_T changed greatly in intertidal pools, reaching maximum values of 9.0 during the day and minimum values of 7.4 during night periods, i.e. a diel range of ca. 1.6 pH_T units. Diel pH_T fluctuations in the surface waters of the adjacent shore were much smaller (8.0–

8.5) but still high, reflecting the metabolic activity of the intertidal vegetation growing on the shore (Fig. 9). The difference in pH between vegetated intertidal pools and adjacent shores provided an additional example of variability in pH between adjacent habitats. Data are available in digital form (Krause-Jensen et al., 2015).

4 Discussion

Our results highlight the nested scales of variability of pH present in the Kobbefjord ecosystem involving (1) seasonal variability, largely driven by the phytoplankton spring bloom as a major event affecting pH, (2) diel variability acting through complex changes in submarine irradiance modulating rates of photosynthesis and respiration of benthic vegetation driven by the interaction of the solar and the tidal cycles, (3) large-scale variability along horizontal and vertical fjord gradients reflecting gradients in metabolic activity in combination with movement of water masses, (4) variability between subtidal habitats with and without kelp forests and between vegetated tidal pools and adjacent vegetated shores reflecting variable degrees of biological control, (5) small-scale three dimensional variability due to heterogeneity in metabolic processes and mixing in vegetated habitats, and (6) micro-scale variability across the boundary layers of macrophytes (Fig. 10).

Overall, metabolic processes played a fundamental role in driving pH-variability across scales, as reflected in strong relationships between oxygen concentration and pH at the fjord-scale and at both diel and seasonal scales. Primary producers played a major role in the regulation of pH-variability, both in the pelagic zone where, particularly, the intense spring bloom characteristic of Arctic ecosystems (Takahashi et al., 2003; Sejr et al., 2014) induced high pH in the subsurface layers while respiratory process in the bottom waters reduced pH; and in the nearshore benthic environment where the presence of subtidal kelp forests and intertidal macroalgae induced marked spatial and diurnal variability in pH. The mosaics of pH reflected that the density of the primary producers, and the spatio-temporal separation of photosynthesis and ecosystem respiration in combination with mixing of water masses were key drivers of the variability in both planktonic and benthic communities. Thus, the vertical gradient of declining pH from upper illuminated to lower shaded habitats varied from the 10–100 m scale in the planktonic community to the m scale in the dense kelp forest.

The scale of seasonal pH-variability in the planktonic community (Fig. 10) compared well with previous reports for the Arctic, showing the spring bloom as a prevalent driver of $p\mathrm{CO}_2$ (Sejr et al., 2011; Meire et al., 2014). The diel variability in kelp beds was in range with that reported from a Californian kelp forest (Frieder et al., 2012), while greater than reported for Mediterranean seagrass beds (Hendriks et al., 2014), and below the range of up to 1 pH unit reported for dense algal mats (Middelboe and Hansen, 2007). The diel variability in pH in the kelp forest was subjected to a stronger direct biological control than that of the microalgae/filamentous algae, as reflected in stronger pH vs. O_2 relationships and steeper pH vs. light relationships, because of the larger density of the kelps and associated faster rates of metabolic activity per unit volume in combination with reduced flow in the dense habitat. The habitat colonized by microalgae/filamentous algae carried a less distinct biological signal reflecting the benthic primary producers at the site in combination with a signal from the planktonic community and the nearby kelp forests in the water masses exchanged with tidal currents. The marked biological control of pH in kelp forests suggests that diel pH may be even more pronounced during sunny days with more intense photosynthesis than during the generally overcast conditions of our survey. Thus, while the identified pH-range and pH vs. O_2-relationships for the planktonic community covered the full growth season, they solely represented a few overcast September days in the benthic habitats and would likely involve markedly higher levels had they covered the full growth season. For sub-Antarctic giant kelp forests, the diel amplitude in $p\mathrm{CO}_2$ and C_T (Delille et al., 2009) during productive periods as well as the seasonal amplitude in pH, C_T and $p\mathrm{CO}_2$ (Delille et al., 2000) were reported to be markedly higher within the kelp forest as compared with unvegetated habitats, underlining the kelps' strong biological control of pH.

We further show, for the first time, significant 3-d variability in pH within 1 m^3 of kelp forest, with pH ranging about 0.2–0.3 pH units at any one point in time and a total variability across deployments of 7.76–8.36 pH_T, resembling the range recorded across the entire growth season in the pelagic. Levels of pH were dependent on the position in the kelp canopy, with the highest pH generally appearing at the top of the canopy and decreasing toward the seafloor, likely reflecting the vertical structure of photosynthetic activity in the kelp bed. Changes in pH were particularly pronounced in small tidal pools, where photosynthesis of dense seaweed stands of primarily *Ascophyllum nodosum* and *Fucus spp.* drove O_2 levels to heavy super saturation (176 %) and forced pH to extremes of up to pH_T 9.0 at low tide during sunny days, corresponding to Ω_{arag} of 4.14 and pCO_2 of 13 µatm compared to night-values of pH_T 7.4, Ω_{arag} of 0.27 and pCO_2 of 1647 µatm driven by community respiration which almost depleted O_2 in the pools (11 % saturation). In surface waters of adjacent densely vegetated intertidal shores, we observed a maximum pH_T of 8.5 with corresponding Ω_{arag} 2.23 and pCO_2 of 96 µatm during the day and a minimum pH_T of 8.0, with corresponding Ω_{arag} of 0.54 and pCO_2 of 243 µatm during the night. While intertidal brown macroalgae thrive in such habitats when regularly flushed as in the current study, apparently only *Ulva (Enteromorpha) intestinalis* occurs in isolated, rarely flushed rock pools where it can drive pH to levels > 10 (Björk et al., 2004).

At the micro-scale, pH also showed considerable variability with a range of up to 0.85 pH units across the boundary layer of the key species of the vegetated shallow ecosystems, with high pH levels at the tissue surface declining towards the bulk water during day time (Fig. 8). There was substantial variability among species, with intertidal macroalgae (*Ascophyllum* and *Fucus*) showing the largest pH range. This microscale pH variability across boundary layers compared well previous observations for the calcifying alga *Hamelida discoidea* (pH-range across boundary layer of 0.7, de Beer and Larkum, 2001) as well as for the coralline algae *Sporolithon durum* (light-dark pH change at tissue surface 0.9; Hurd et al., 2011; Roleda and Hurd, 2012) and *Arthrocardia corymbosa* (pH range across boundary layer e.g. 0.4, depending on flow; Cornwall et al., 2013). The boundary layer thickness as well as the pH range across it depends markedly on flow conditions. Reduced flows as present in dense vegetation increase the boundary layer thickness and consequently the pH range (Hurd et al., 2011; Cornwall et al., 2013). Exchange of water masses with different salinity and temperature also added to the variability in pH as indicated for both pelagic (Fig. 3b) and benthic (Fig. 4) systems but showed much weaker correlation to pH than did O_2 concentrations reflecting the biological control.

The processes above resulted in nested scales of pH variability in the Kobbefjord ecosystem (Fig. 10), with variability ranging 0.2–0.85 units across spatial scales and 0.2–1.6 units over diurnal to seasonal scales. This variability provides a dynamic mosaic of niches for organisms. Niches of high pH may be particularly important for the more vulnerable larval and juveniles stages of calcifiers under acidic conditions as projected for the future (Kroecker et al., 2013). The suitability for calcifiers is best represented by Ω_{arag}, where calcifiers should be favored by high Ω_{arag} values. The Kobbefjord ecosystems host a number of calcifying species, including bivalves such as blue mussel, scallops and snails, echinoderms, such as green sea urchins, and crustaceans such as *Pseudobalanus balanoides*, calcareous algae and foraminifers. Overall, the identified Ω_{arag} conditions were favorable to calcification as they were generally well above 1, particularly in illuminated habitats with intense photosynthesis. The phytoplankton spring bloom, depleting CO_2 and driving Ω_{arag} to values close to 3, would also provide adequate conditions for pelagic calcifiers, as it would provide the double benefit of adequate environments for aragonite deposition and food supply to support growth and the energetic demands of calcifiers. Canopies of kelp and intertidal seaweed environments may also provide adequate niches for calcifiers during summer, when Ω_{arag} values would be highest through the cumulative action of the processes upregulating pH and Ω_{arag} values discussed above. Indeed, most calcifiers spawn and recruit in early summer (Arendt et al., 2013) when $p\mathrm{CO}_2$ remains low, warmer water temperatures lead to higher Ω_{arag} and high solar radiation and long photoperiod allow seaweeds to draw down CO_2 further (Delille et al., 2000).

The upregulating effect of primary producers on pH is counterbalanced by the opposite effect of respiration and decomposition prevailing in shaded and deeper basins and periods as illustrated by the large scale seasonal variability in the pelagic community (Fig. 2), and paralleled in kelp forests outside the productive period (Delille et al., 2009) as well as during night time and in shaded layers of the kelp forest (Fig. 7) and tidal pools (Fig. 9). These shaded habitats with diurnally low Ω_{arag} could be challenging habitats for calcifyers. Interestingly, however, blue mussels grew in close association with macroalgae even in intertidal pools, where they would experience maximum Ω_{arag} values of up to 4.28 when low tide occurred at noon as opposed to levels as low as 0.28 during night (Fig. 9). Blue mussels have indeed been observed to abound in intertidal macroalgal habitats (Blicher et al., 2013) and along with other calcifiers to be trophically linked with habitat-forming algae such as *Ascophyllum* (Riera et al., 2009). Probably the recurring periods of high Ω_{arag} in combination with adequate food supply can compensate for the potential problems of low Ω_{arag} during night. Laboratory experiments have demonstrated that semidiurnal fluctuations of 0.3 pH units may compensate for negative effects of constantly low pH on the development of mussel larvae (Frieder et al., 2014). Calcareous epiphytic organisms, such as encrusted algae and bryozoans would also experience high variability in Ω_{arag} at the surface of the plant tissue, where periodically high Ω_{arag} values favors calcification, as elegantly demonstrated by de Beer and Larkum (2001).

The existence of a mosaic of environments in the Kobbefjord underlines the importance of metabolic processes along with habitat configuration and interactions among community constituents in affecting pH in coastal ecosystems as opposed to the simpler situation in the open ocean (Duarte et al., 2013; Hendriks et al., 2014). This pronounced influence of metabolic processes occurs in spite of Kobbefjord being a macrotidal area with marked exchange of water masses with the coastal region and is probably also the case in many other shallow coastal areas in the Arctic, as has also been highlighted for areas in the temperate zone (Duarte et al., 2013). While the current study explored pH in benthic habitats under overcast situations in the early autumn of the sub-Arctic, kelp forests are likely to induce much more pronounced increases in pH and Ω_{arag} in midsummer when irradiances are higher and the photoperiod longer, and further north, during high-Arctic midsummer, when the sun does not set for months. Under scenarios of ocean acidification such coastal environments of increased primary production should gain increased importance as local refuges for calcifyers. The projected poleward expansion of macrophytes into the Arctic with warming and reduced sea ice cover (Müller et al., 2009; Jueterbock et al., 2013) has been hypothesized to provide such niches of elevated pH and Ω_{arag} during summer (Krause-Jensen et al., 2014). Similarly, increased pelagic primary production has been forecasted for parts of the Arctic Ocean (Arrigo et al., 2008; Slagstad et al., 2011; Popova et al., 2012) and may also gain increased importance as local niches of high pH.

Author contributions. Planning, field work, data processing and writing were carried out jointly, led by D. Krause-Jensen and C. M. Duarte, with L. Meire and M. K. Sejr responsible for fjord-scale surveys, I. E. Hendriks, M. K. Sejr, M. E. Blicher, C. M. Duarte and D. Krause-Jensen responsible for the various small scale measurements, I. E. Hendriks and N. Marbà for micro-scale measurements, N. Marbà and D. Krause-Jensen for intertidal measurements and M. E. Blicher for Greenland field facilities. Main idea: C. M. Duarte.

Acknowledgements. The study was funded by the Danish Environmental Protection Agency within the Danish Cooperation for Environment in the Arctic (DANCEA). L. Meire was funded by the Research foundation Flanders (FWO aspirant grant) and by Defrost under the Nordic Centers of Excellence (NCoE) program. O. Geertz-Hansen, Greenland Climate Research Centre,/Greenland Institute of Natural Resources, Nuuk, is thanked for help with field work. The study is also a contribution to the Greenland Ecosystem Monitoring program (www.G-E-M.dk) and the Arctic Science Partnership (ASP) asp-net.org.

References

AMAP: AMAP Assessment 2013: Arctic Ocean Acidification, Arctic Monitoring and Assessment Programme (AMAP), Oslo, Norway, viii + 99 pp., ISBN–978-82-7971-082-0, 2013.

Arendt, K. E., Juul-Pedersen, T., Mortensen, J., Blicher, M. E., and Rysgaard, S: A 5-year study of seasonal patterns in mesozooplankton community structure in a sub-Arctic fjord reveals dominance of *Microsetella norvegica* (Crustacea, Copepoda), J. Plankton Res., 35, 105–120, doi:10.1093/plankt/fbs087, 2013.

Arrigo, K. R., van Dijken, G., and Pabi, S.: Impact of a shrinking Arctic ice cover on marine primary production, Geophys. Res. Lett., 35, 1–6, 2008.

Attard, K. M., Glud, R. N., McGinnis, D. F., and Rysgaard, S.: Seasonal rates of benthic primary production in a Greenland fjord measured by aquatic eddy correlation, Limnol. Oceanogr., 59, 1555–1569, 2014.

Blicher, M. E. and Sejr, M. K.: Abundance, oxygen consumption and carbon demand of brittle stars in Young Sound and the NE Greenland shelf, Mar. Ecol.-Prog. Ser., 422, 139–144, doi:10.3354/meps08915, 2011.

Blicher, M. E., Rysgaard, S., and Sejr, M. K.: Growth and production of sea urchin Strongylocentrotus droebachiensis in a high-Arctic fjord, and growth along a climatic gradient (64 to 77 degrees N) (vol 341, pg 89, 2007), Mar. Ecol. Ser., 341, 89–102, 2007.

Blicher, M. E., Sejr, M. K., and Rysgaard, S.: High carbon demand of dominant macrozoobenthic species indicates their central role in ecosystem carbon flow in a sub-Arctic fjord, Mar. Ecol. Ser., 383, 127–140, doi:10.3354/meps07978, 2009.

Blicher, M. E., Rasmussen, L. M., Sejr, M. K., Merkel, F. R., and Rysgaard, S.: Abundance and energy requirements of eiders (*Somateria spp.*) suggest high predation pressure on macrobenthic fauna in a key wintering habitat in SW Greenland, Polar Biol., 34, 1105–1116, doi:10.1007/s00300-011-0968-3, 2011.

Blicher, M. E., Sejr, M. K., and Høgslund, S.: Population structure of *Mytilus edulis* in the intertidal zone in a sub-Arctic fjord, SW Greenland, Mar. Ecol.-Prog. Ser., 487, 89–100, 2013.

Björk, M., Axelsson, L., and Beer, S.: Why is *Ulva intestinalis* the only macroalga inhabiting isolated rock pools along the Swedish Atlantic coast?, Mar. Ecol.-Prog. Ser., 284, 109–116, 2004.

Born, E. W., Rysgaard, S., Ehlme, G., Sejr, M., Acquarone, M., and Levermann, N.: Underwater observations of foraging free-living Atlantic walruses (*Odobenus rosmarus rosmarus*) and estimates of their food consumption, Polar Biol., 26, 348–357, 2003.

Cornwall, C. E., Hepburn, C. D., Pritchard, D., Currie, K. I., McGraw, C. M., Hunter, K. A., and Hurd, C. L.: Carbon use-strategies in macroalgae: differential responses to lowered pH and implications for ocean acidification, J. Phycol., 48, 137–144, doi:10.1111/j.1529-8817.2011.01085.x, 2012.

De Beer, D. and Larkum, A. W. D.: Photosynthesis and calcification in the calcifying algae *Halimeda discoidea* studied with microsensors, Plant Cell Environ., 24, 1209–1217, 2001.

Delille, B., Delille, D., Fiala, M., Prevost, C., and Frankignoulle, M.: Seasonal changes of $p\mathrm{CO}_2$ over a subantarctic Macrocystis kelp bed, Polar Biol., 23, 706–716, 2000.

Delille, B., Borges, A. V., and Delille, D.: Influence of giant kelp beds (*Macrocystis pyrifera*) on diel cycles of $p\mathrm{CO}_2$ and DIC in the sub-Antarctic coastal area, Estuar. Coast. Shelf S., 81, 114–122, doi:10.1016/j.ecss.2008.10.004, 2009.

Dickson, A. G. and Millero, F. J.: A comparison of the equilibrium constants for the dissociation of carbonic acid in seawater media, Deep-Sea Res., 34, 1733–1743, 1987.

Dickson, A. G., Sabine, C. L., and Christian, J. R.: Guide to Best Practices For Ocean CO_2 Measurements, PICES Special Publication, 191 pp., 2007.

Duarte, C., Hendriks, I., Moore, T., Olsen, Y., Steckbauer, A., Ramajo, L., Carstensen, J., Trotter, J., and McCulloch, M.: Is ocean acidification an open-ocean syndrome?, understanding anthropogenic impacts on seawater pH, Estuar. Coast., 36, 221–236, 2013.

Fabry, V. J., McClintock, J. B., Mathis, J. T., and Grebmeier, J. M.: Ocean acidification at high latitudes, The Bellweather. Oceanogr., 22, 160–171, 2009.

Frieder, C. A., Nam, S. H., Martz, T. R., and Levin, L. A.: High temporal and spatial variability of dissolved oxygen and pH in a nearshore California kelp forest, Biogeosciences, 9, 3917–3930, doi:10.5194/bg-9-3917-2012, 2012.

Frieder, C. A., Gonzales, J. P., Bockmon, E. E., Navarro, M. O., and Levini, L. A.: Can variable pH and low oxygen moderate ocean acidification outcomes for mussel larvae?, Glob. Change Biol., 20, 754–764, doi:10.1111/gcb.12485, 2014, 2014.

Glud, R. N., Berg, P., Hume, A., Batty, P., Blicher, M. E., Lennert, K., and Rysgaard, S.: Benthic O_2 exchange across hard-bottom substrates quantified by eddy correlation in a sub-Arctic fjord, Mar. Ecol.-Prog. Ser., 417, 1–12, doi:10.3354/meps08795, 2010.

Helm, V., Humbert, A., and Miller, H.: Elevation and elevation change of Greenland and Antarctica derived from CryoSat-2, The Cryosphere, 8, 1539–1559, doi:10.5194/tc-8-1539-2014, 2014.

Hendriks, I. E., Olsen, Y. S., Ramajo, L., Basso, L., Steckbauer, A., Moore, T. S., Howard, J., and Duarte, C. M.: Photosynthetic activity buffers ocean acidification in seagrass meadows, Biogeosciences, 11, 333–346, doi:10.5194/bg-11-333-2014, 2014.

Hofmann, G. E., Smith, J. E., Johnson, K. S., Send, U., Levin, L. A., Micheli, F., Paytan, A., Price, N. N., Peterson, B., Takeshita, Y., Matson, P. G., Crook, E. D., Kroeker, K. J., Gambi, M. C., Rivest, E. B., Frieder, C. A., Yu, P. C., and Martz, T. R.: High-frequency dynamics of ocean ph: a multi-ecosystem comparison, PLoS ONE, 6, e28983, doi:10.1371/journal.pone.0028983, 2011.

Hurd, C. L., Cornwall, C. E., Currie, K., Hepburn, C. D., McGraw, C. M., Hunter, K. A., and Boyd, P. W.: Metabolically-induced pH fluctuations by some coastal calcifiers exceed projected 22nd century ocean acidification: a mechanism for differential susceptibility?, Glob. Change Biol., 17, 3254–3262, doi:10.1111/j.1365-2486.2011.02473.x, 2011.

Høgslund, S., Sejr, M. S., Wiktor Jr., J., Blicher, M. E., and Wegeberg, S.: Intertidal community composition along rocky shores in Southwest Greenland: a quantitative approach, Polar Biol., 37, 1549–1561, doi:10.1007/s00300-014-1541-7, 2014.

Jueterbock, A., Tyberghein, L., Verbruggen, H., Coyer, J. A., Olsen, J. L., and Hoarau, G.: Climate change impact on seaweed meadow distribution in the North Atlantic rocky intertidal, Ecol. Evol., 3, 1356–1373, doi:10.1002/ece3.541, 2013.

Krause-Jensen, D. and Duarte, C. M. Expansion of vegetated coastal ecosystems in the future Arctic, Front. Mar. Sci., 1, 77, doi:10.3389/fmars.2014.00077, 2014.

Krause-Jensen, D., Marbà, N., Olesen, B., Sejr, M. K., Christensen, P. B., Rodrigues, J., Renaud, P. E., Balsby, T. J. S., and Rysgaard, S.: Seasonal sea ice cover as principal driver of spatial and temporal variation in depth extension and annual production of kelp in Greenland, Glob. Change Biol., 18, 2981–2994, 2012.

Krause-Jensen, D., Duarte, C. M., Hendriks, I. E., Meire, L., Blicher, M. E., Marbà, N., and Sejr, M. K.: Nested scales of pH variability in sub-Arctic Kobbefjord, SW Greenland”, DIGITAL.CSIC, available at: http://hdl.handle.net/10261/112946, 2015.

Kroeker, K. J., Kordas, R. L., Crim, R., Hendriks, I. E., Ramajos, L., Singh, G. S., Duarte, C. M., and Gattuso, J.-P.: Impacts of ocean acidification on marine organisms: quantifying sensitivities and interaction with warming, Glob. Change Biol., 19, 1884–1896, doi:10.1111/gcb.12179, 2013.

Mehrbach, C., Culberson, C. H., Hawley, J. E., and Pytkowicz, R. M.: Measurement of the apparent dissociation constants of carbonic acid in seawater at atmospheric pressure, Limnol. Oceanogr., 18, 897–907, 1973.

Meire, L., Søgaard, D. H., Mortensen, J., Meysman, F. J. R., Soetaert, K., Arendt, K. E., Juul-Pedersen, T., and Rysgaard, S.: Glacial meltwater and primary production as drivers for strong CO_2 uptake in fjord and coastal waters adjacent to the Greenland Ice Sheet, Biogeosciences Discuss., 11, 17925–17965, doi:10.5194/bgd-11-17925-2014, 2014.

Middelboe, A. L. and Hansen, P. J.: Direct effects of pH and inorganic carbon on macroalgal photosynthesis and growth, Mar. Biol. Res., 3, 134–144, 2007.

Müller, R., Laepple, T., Bartsch, I., and Wiencke, C. Impact of oceanic warming on the distribution of seaweeds in polar and cold-temperate waters, Bot. Mar., 52, 617–638, doi:10.1515/BOT.2009.080, 2009.

Olesen, B., Krause-Jensen, D., Marbà, N., and Christensen, P. B.: Eelgrass (*Zostera marina* L.) meadows in subarctic Greenland: dense meadows with slow biomass turnover, Mar. Ecol.-Prog. Ser., 518, 107–121, doi:10.3354/meps11087, 2015.

Pierrot, D. E. L. and Wallace, D. W. R.: MS Excel Program Developed for CO_2 System Calculations, ORNL/CDIAC-105a, Carbon Dioxide Information Analysis Center, Oak Ridge National Laboratory, U. S. Department of Energy, Oak Ridge, Tennessee, doi:10.3334/CDIAC/otg.CO2SYS_XLS_CDIAC105a, 2006.

Popova, E. E., Yool, A., Coward, A. C., Dupont, F., Deal, C., Elliott, S., Hunke, E., Jin, M., Steele, M., and Zhang, J.: What controls primary production in the Arctic Ocean? Results from an intercomparison of five general circulation models with biogeochemistry, J. Geophys. Res., 117, C00D12, doi:10.1029/2011JC007112, 2012.

Riera, P., Escaravage, C., and Leroux, C.: Trophic ecology of the rocky shore community associated with the Ascophyllum nodosum zone (Roscoff, France): a δ^{13}C vs. δ^{15}N investigation, Estuar. Coast. Shelf S., 81, 143–148, 2009.

Richter, A., Rysgaard, S., Dietrich, R., Mortensen, J., and Petersen, D.: Coastal tides in West Greenland derived from tide gauge records, Ocean Dynam., 61, 39–49, doi:10.1007/s10236-010-0341-z, 2011.

Roleda, M. Y. and Hurd, C. L.: Seaweed responses to ocean acidification, in: Seaweed Biology, Ecological Studies, 219, edited by: Wiencke, C. and Bischof, K., Springer-Verlag, Berlin, Heidelberg, 407–431, ISBN 978-3-642-28450-2.xiii, 510 pp., 2012.

Sejr, M. K., Sand, M. K., Jensen, K. T., Petersen, J. K., Christensen, P. B., and Rysgaard, S.: Growth and production of Hiatella arctica (Bivalvia) in a high-Arctic fjord (Young Sound, Norhteast Greenland), Mar. Ecol.-Prog. Ser., 244, 163–169, 2002.

Sejr, M. K., Krause-Jensen, D., Rysgaard, S., Sørensen, L. L., Christensen, P. B., and Glud, R. N.: Air–sea flux of CO_2 in arctic coastal waters influenced by glacial melt water and sea ice, Tellus B, 63, 815–822, doi:10.1111/j.1600-0889.2011.00540.x, 2011.

Sejr, M. K., Krause-Jensen, D., Dalsgaard, T., Ruiz-Halpern, S., Duarte, C. M., Middelboe, M., Glud, R. N., Bendtsen, J., and Rysgaard, S.: Seasonal dynamics of autotrophic and heterotrophic plankton metabolism and $p\mathrm{CO}_2$ in a subarctic Greenland fjord, Limnol. Oceanogr., 59, 1764–1778, 2014.

Slagstad, D., Ellingsen, I. H., and Wassmann, P.: Evaluating primary and secondary production in an Arctic Ocean void of summer sea ice: an experimental simulation approach, Prog. Oceanogr., 90, 117–131, doi:10.1016/j.pocean.2011.02.009, 2011.

Takahashi, T., Olafsson, J., Goddard, J. G., Chipman, D. W., and Sutherland, S. C.: Seasonal variation of CO_2 and nutrients in the high-latitude surface oceans: a comparative study, Global Biogeochem. Cy., 7, 843–878, 1993.

Uppström L. R.: The boron/chlorinity ratio of deep-sea water from the Pacific Ocean, Deep-Sea Res., 21, 161–162, 1974.

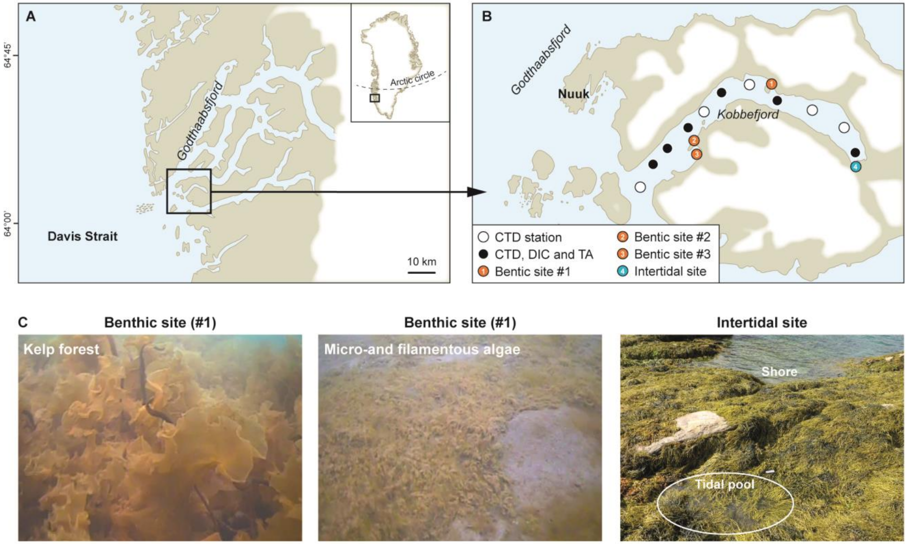

Figure 1. **(a)** Location of Kobbefjord, Nuuk. **(b)** Location of sampling sites in Kobbefjord: Fjord scale sites (CTD, C_T, A_T: filled circles; CTD: open circles), vegetated subtidal sites (open circles # 1–3), and intertidal sites (open circles (#4). **(c)** Photopanel of benthic habitats: a typical kelp forest habitat and habitat colonized by microalgae/scattered filamentous algae (example from site # 1, representative of sites # 1–3 in map) and a vegetated intertidal pool and the adjacent vegetated shore (site # 4 in map).

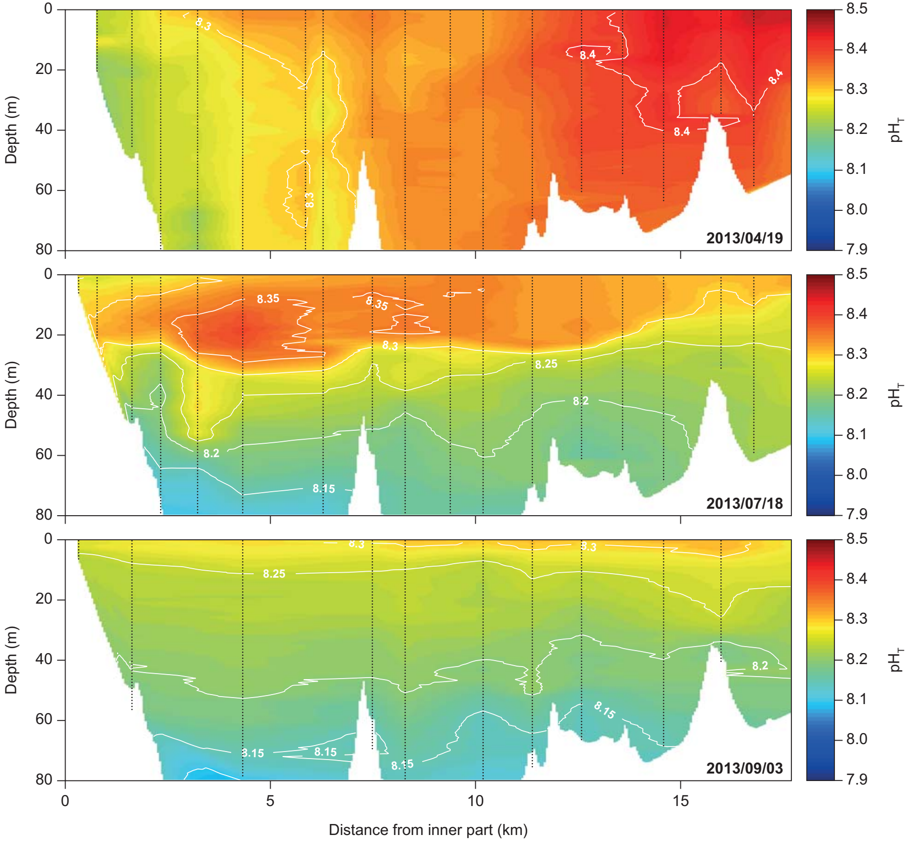

Figure 2. Fjord-scale pH-variability in Kobbefjord 19 April, 18 July and 3 September 2013.

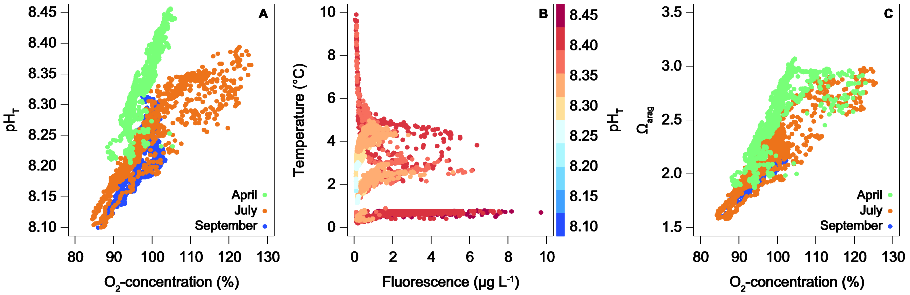

Figure 3. Fjord-scale relationships in Kobbefjord between pH and oxygen **(a)**, temperature and fluorescence with associated pH-levels shown with symbol color **(b)**, and pH and Ω_{arag} **(c)**, based on three sampling occasions: 19 April, 18 July and 3 September 2013.

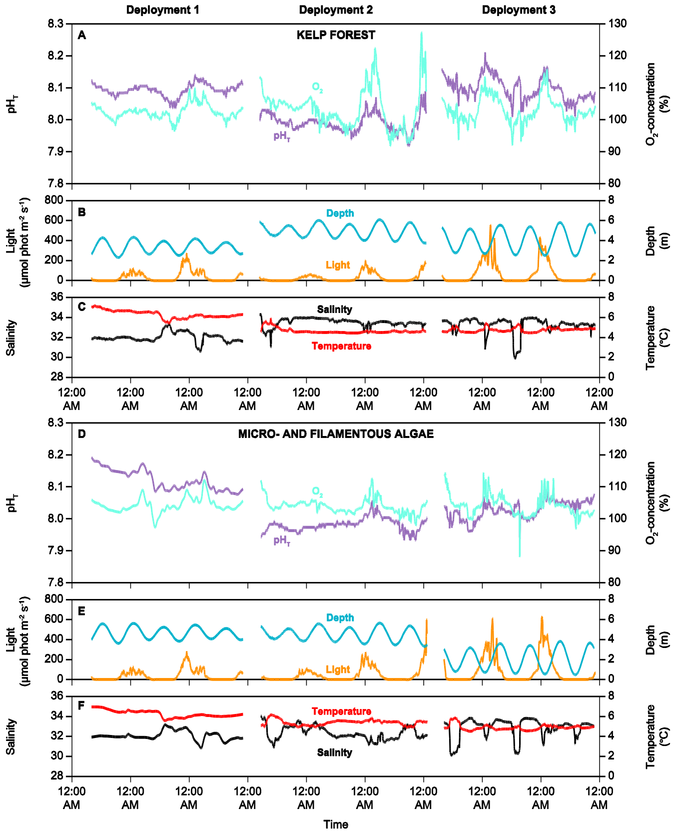

Figure 4. Diurnal variability in pH, O_2, water depth (all measured by Hydrolab) and light (measured by Odyssey loggers) at ca. 50 cm above the seafloor in kelp forests **(a–c)** and habitats colonized by microalgae/filamentous algae **(e–f)** during three parallel deployment in Kobbefjord, Nuuk, 27–30 August, 30 August–2 September, 2–5 September 2013. The deployments represent the benthic sites (# 1–3, respectively) shown on the map (Fig. 1).

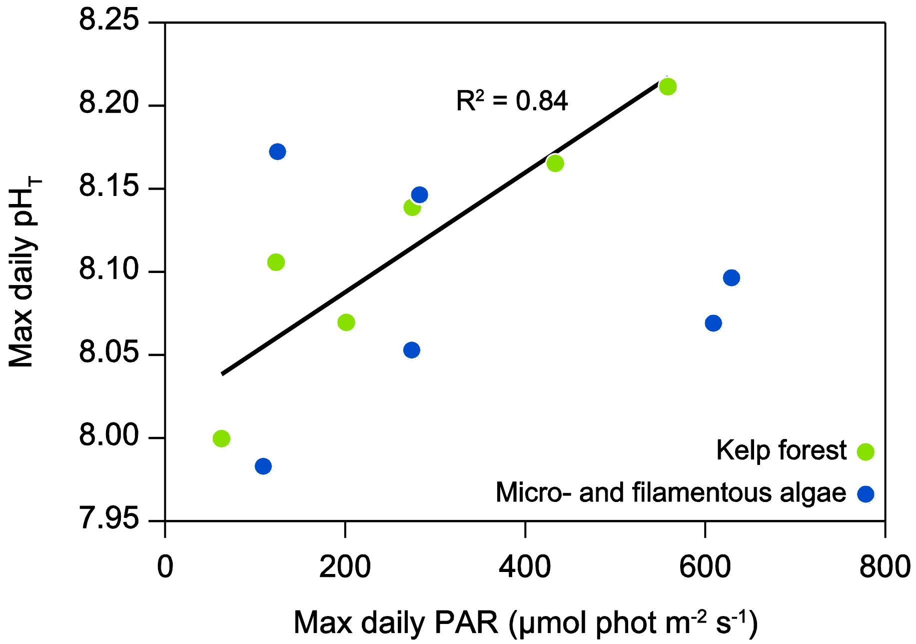

Figure 5. Maximum daily pH in a kelp forest (green dots) and above microalgae/filamentous algae (blue dots) as a function of maximum daily incident light over 6 full days as measured during three parallel deployment in Kobbefjord, Nuuk, 27–30 August, 30 August–2 September, 2–5 September 2013. Linear fit and coefficient of determination shown for the significant relationship for the kelp forest.

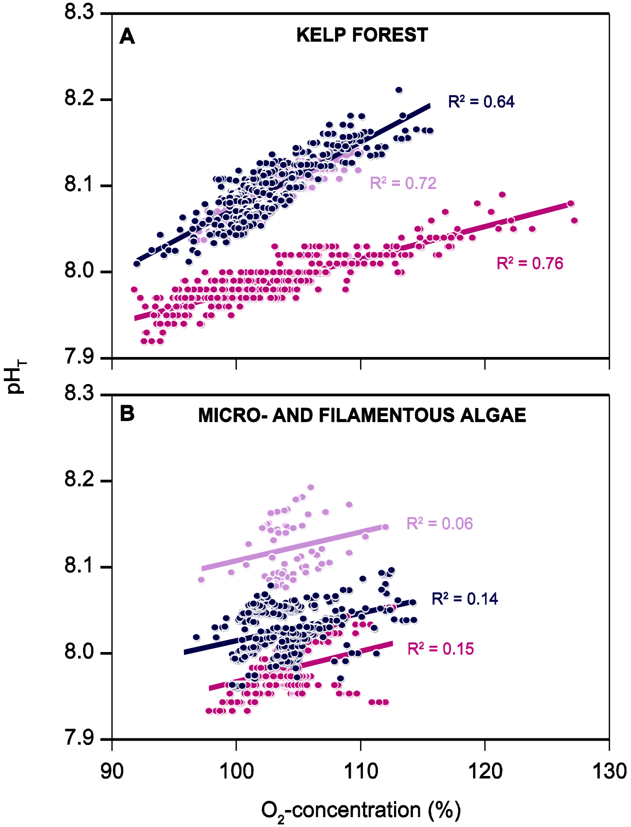

Figure 6. pH vs. O_2 concentration for three parallel deployments (# 1–3 shown by increasing color intensity) in subtidal habitats colonized by kelp forests (top panel) or microalgae/scattered filamentous algae (bottom panels) in Kobbefjord, Nuuk, August–September 2013. Each deployment represents 10 min loggings by multiloggers (Hydrolab) over ca. 2 diurnal cycles. Linear fits and coefficients of determination are shown.

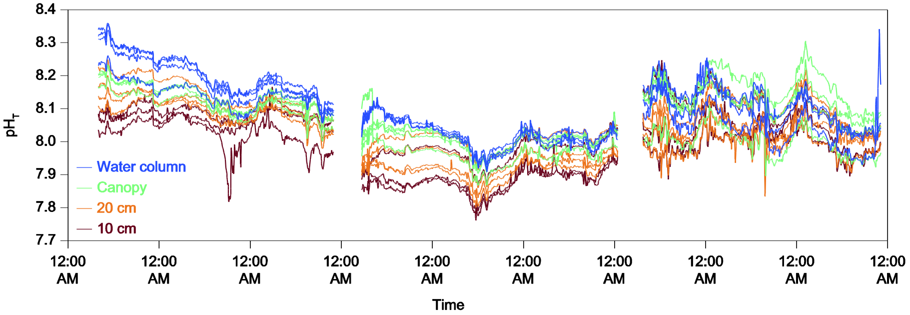

Figure 7. pH-variability within 1 m^3 of kelp forest in Kobbefjord, Nuuk, during three deployments in late August–September 2013. 16 pH-sensors were configured in-situ in a 3-d array with 4 sensors at 0.1 m from the bottom, 4 sensors at 0.2 m, 4 sensors just underneath the canopy and 4 in the water column above the canopy, which typically extended about 0.75 m above the seafloor.

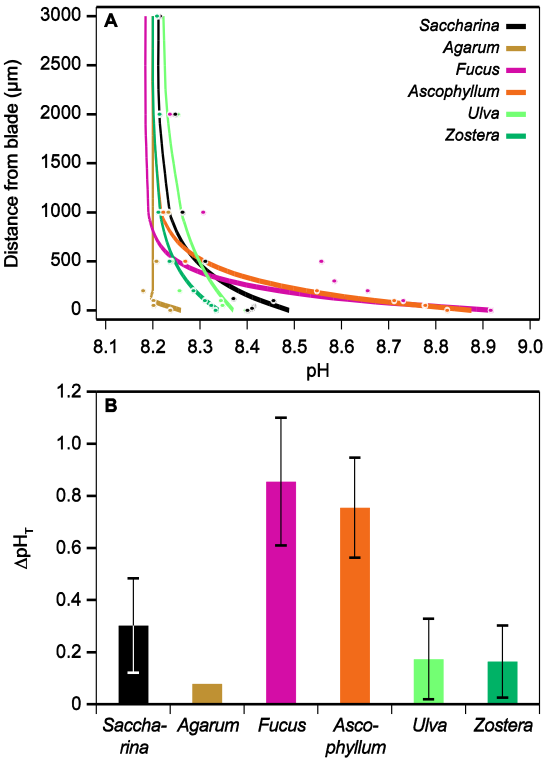

Figure 8. Microscale pH-variability across boundary layers of blades of 6 different macrophyte species illuminated by 200 µmol photons $m^{-2} s^{-1}$: the kelps *Saccharina latissima* and *Agarum clathratum*, the intertidal brown macroalgae: *Fucus vesiculosus* and *Ascophyllum nodosum*, the green macroalga *Ulva lactuca* and the seagrass *Zostera marina*. **(a)** pH levels (mean of 2–3 replicate measurements) across blade boundary layers fitted by an exponential model ($y = y0 + a \times \exp^{-b \times x}$, $R^2 > 0.90$ for all individual fits). **(b)** pH range across the boundary layer of the various species.

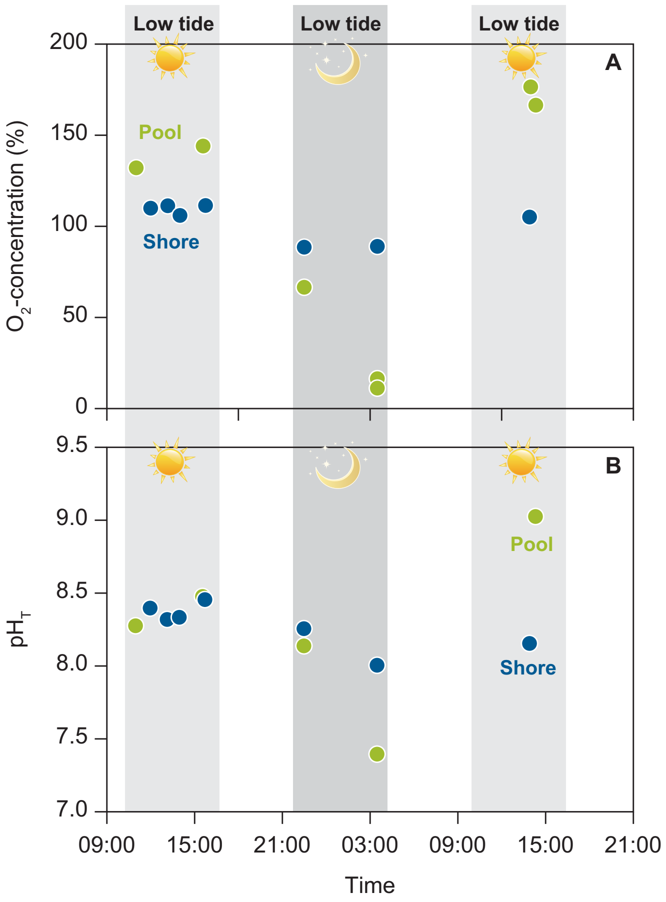

Figure 9. O_2-concentration and pH in vegetated tidal pools and in surface waters of neighboring vegetated intertidal shores measured at low tide during day and night just after pool formation and before pool inundation.

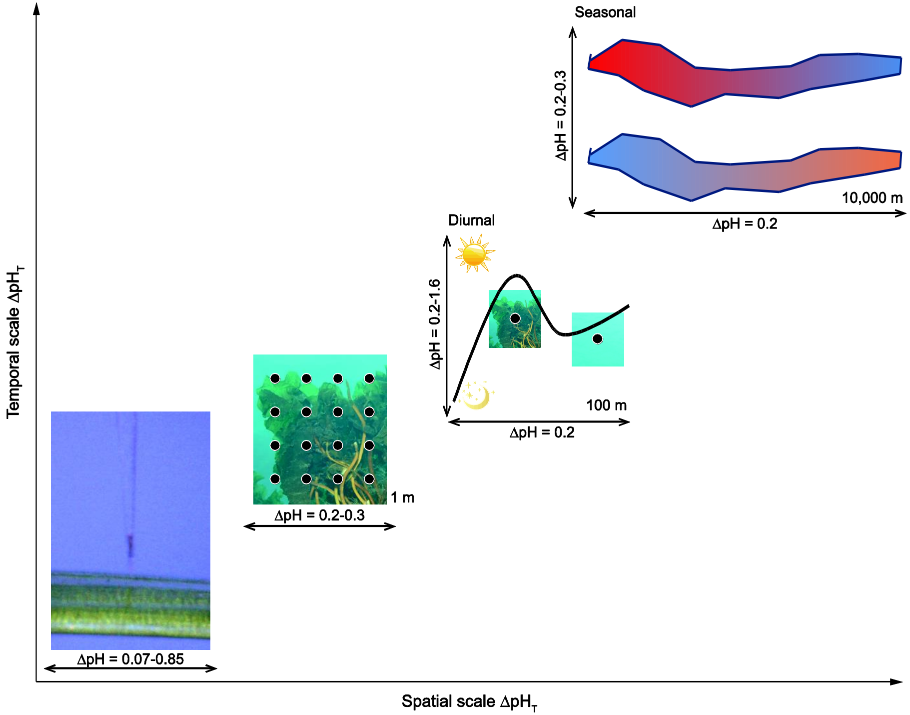

Figure 10. Conceptual summary of nested scales of temporal and spatial variability in pH in Kobbefjord, Nuuk. The figure shows the maximum pH range at the various scales examined. From lower left to upper right: (1) micro-scale variability across macrophyte boundary layers, (2) small scale variability within kelp forests, (3) diurnal variability in vegetated subtidal habitats and intertidal pools/adjacent shores and variability between habitats at the 100 m scale, (4) seasonal and fjord-scale horizontal variability.

Title Page
Abstract | Introduction
Conclusions | References
Tables | Figures
◀| |▶
◀ ▶
Back | Close
Full Screen / Esc
Printer-friendly Version
Interactive Discussion

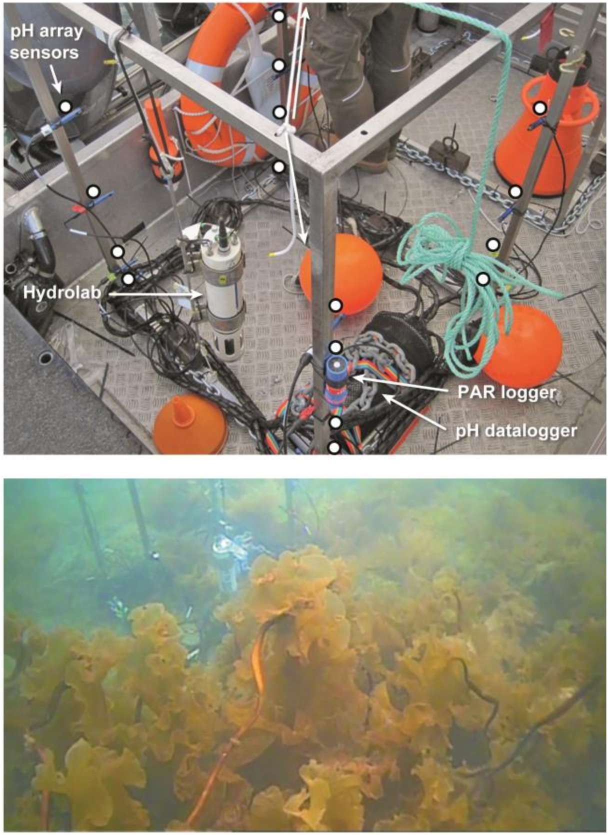

Figure A1. Photo of deployment frame with loggers shown on the deck of the boat (upper panel) and in situ in the kelp forest (site # 1, central panel). Markings in upper panel show the array of 16 pH sensors connected to a common pH logger, the hydrolab measuring salinity, temperature and oxygen and a PAR logger (odyssey).

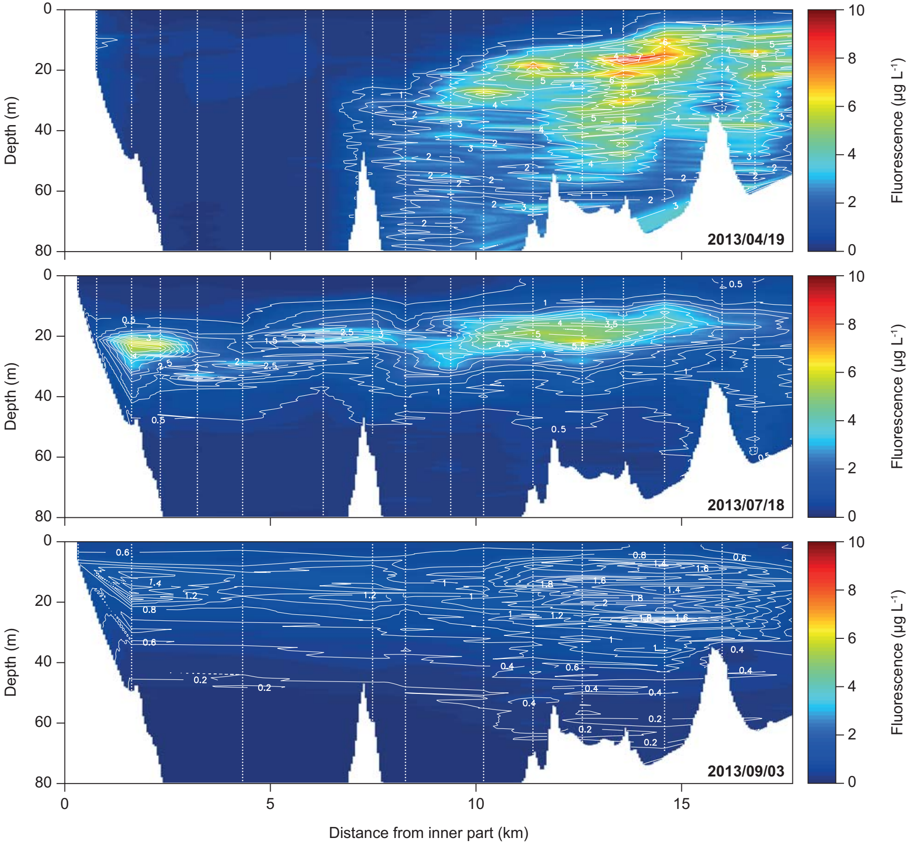

Figure A2. Fjord-scale variability in fluorescence in Kobbefjord, Nuuk, 19 April, 18 July and 3 September 2013.

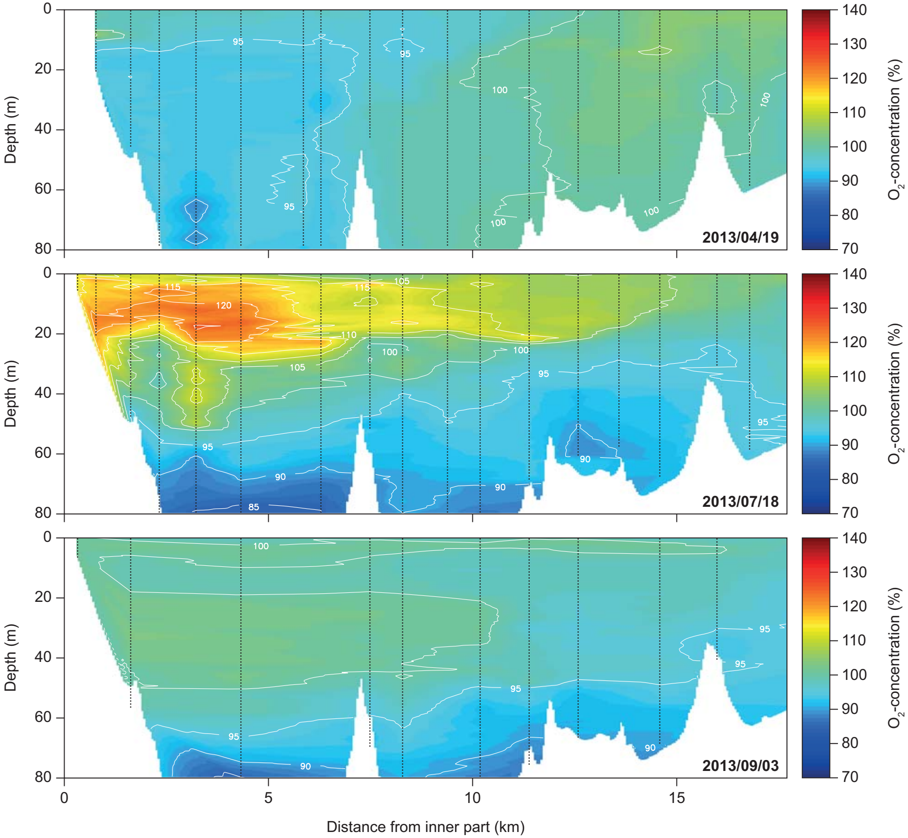

Figure A3. Fjord-scale variability in O_2-concentration in Kobbefjord, Nuuk, 19 April, 18 July and 3 September 2013.

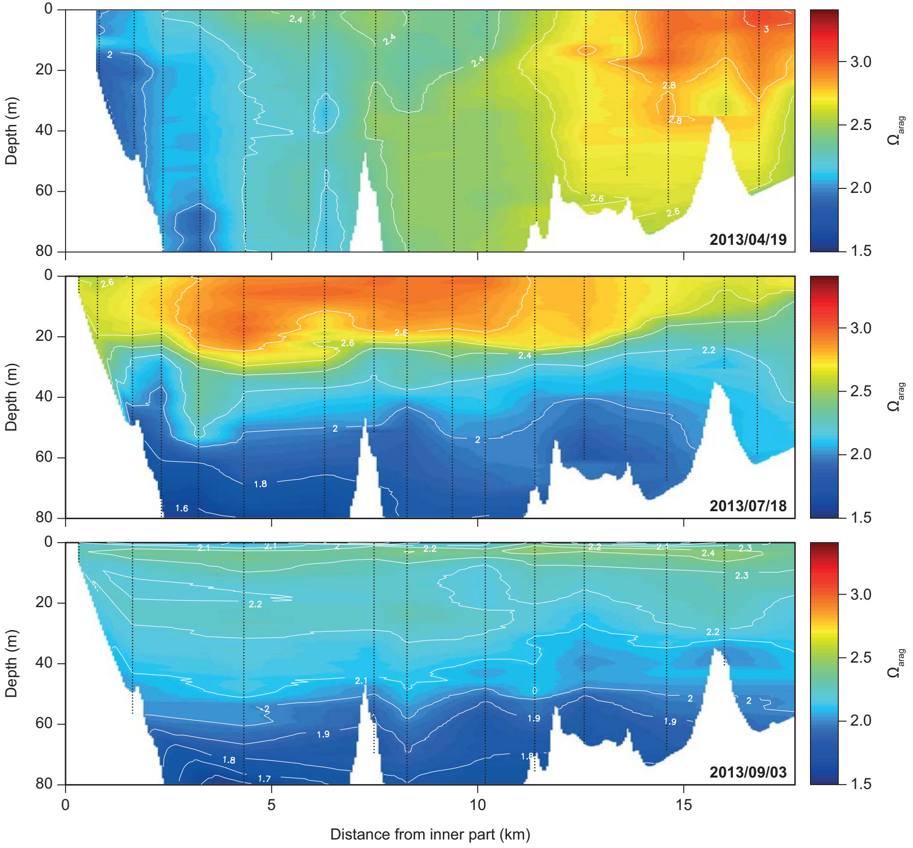

Figure A4. Fjord-scale variability in Ω_{arag} in Kobbefjord, Nuuk, 19 April, 18 July and 3 September 2013.